

# Comparative Studies on Vibration Reduction Capabilities of Bearings with Squeeze Film Dampers and Active Magnetic Bearings Employed on a Simply Supported Rotor System

R Singaravelu<sup>1</sup>, Nagaraja S N<sup>2</sup>, K Ganesh<sup>3</sup>

<sup>1</sup>PG Student, Dept. Of Mechanical Engineering, Kuppam Engineering college, AP, India

<sup>2</sup>Assistant Professor, Dept. Of Mechanical Engineering, Kuppam Engineering college, AP, India

<sup>3</sup>Associate Professor & HOD, Dept. Of Mechanical Engineering, Kuppam Engineering college, AP, India

\*\*\*

**Abstract** - In this work a comparative study of the vibration reduction capabilities of rolling element bearings provided with external damping and that of magnetic bearings is studied. A simply supported rotor system with two discs and subjected to unbalance force is considered. The rotor system is modeled with Timoshenko beam elements which consider shear deformation and rotational inertia. The global equation of motion of the rotor bearing system is solved in time domain in Mat lab /Simulink environment. Firstly the case of the rotor with two discs supported on two rolling element bearings is considered. Three different clearances are considered in SFD and their effect on vibration reduction is studied. Next the two rolling element bearings are replaced with two active magnetic bearings with 8 poles each. A parametric study of the effect of changing the value of  $k_p$ ,  $k_i$ ,  $k_d$  is performed. Time domain wave forms and orbit plots are used to compare the vibration of the rotor systems for the cases with SFDs and AMBs. It has been observed that AMBs are superior to conventional bearing/damper configuration in terms of vibration suppression capabilities thus making them a good choice for industrial applications

**Key Words:** Active magnetic bearing; Squeeze film damper, Vibration, Bearing

## 1. Introduction

AMBs are used as bearings however unlike conventional bearings there is no contact between stator and rotor. AMBs can produce only attractive forces and therefore a closed loop controller is required to maintain stable operation. AMBs offer various advantages over rolling element bearings such as high speed, tunability, no wear, no lubrication, and lower power consumption.

The working principle of AMB is shown in Fig-1. An AMB system consists of four essential sub systems: magnetic actuator, controller (digital/analog), power amplifier, and proximity probe. When the rotor position changes the signal from proximity probe is sent to controller which sends error signal to power amplifier which in turn sends the necessary current to the actuator coils. The coils create magnetic flux and attract the rotor back to its equilibrium position. This real time process helps in levitating the rotor during its operation.

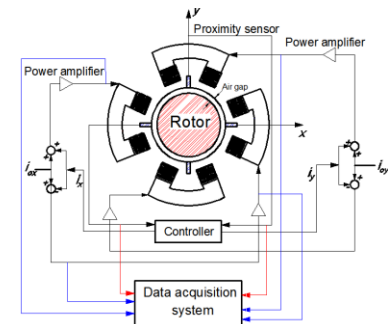


**Fig-1:** Working principle of AMB-rotor system (taken from Srinivas et al., 2018)

In AMB applications, each bearing axis has a pair of power amplifiers. They supply the actuator coils with the current required to generate the forces that act on the rotor. Thus they function between controller and the coils of electromagnetic actuator. Eddy current proximity probes, capacitive sensors, inductive pick-ups, magnetic pick-ups, optical sensors, photo-electric sensors, laser type sensors and Hall sensors are the most commonly used sensors in AMB applications (Schweitzer and Maslen, 2009; Tiwari, 2011). Eddy current sensors have a displacement range of 2 mm and possess good frequency response and are most commonly used. Touch down bearings also called auxiliary or backup or retainer bearings are mounted at one half of AMB air gap to protect the AMB in the event of power failure or load saturation. During normal operation they are not in contact with the rotor.

## 2. Literature Review

Das and Dutt (2010) controlled the transverse vibrations of a flexible rotor-shaft using a combination of PD law and extended state observer. Basaran et al. (2011) used a  $H_\infty$  controller on a flexible rotor supported on two radial AMBs and a thrust AMB to control its vibrations as it passed through the first critical speed. Kozanecka et al. (2011) applied AMB as a vibration damper in the torque transmission system to a tail rotor of a helicopter to pass through three critical speeds.

Zhong and Zhu (2013) tested the steady state response and acceleration response of a flexible rotor using a 2-DOF PID controller as it passed through the first critical speed. The PID controller showed higher damping and better stability than the 1-DOF PID controller. Defoy et al. (2014) compared the performances of a simple PID, SISO fuzzy PID and polar fuzzy controllers on a flexible rotor – AMB test rig.

Wang et al. (2014) used virtual trial-weights method, which simulate the physical trial weights, for field balancing a magnetically levitated flexible rotor below the critical speed. AMBs produce synchronous electromagnetic forces which act as trial weights in this method. Di and Lin (2014) applied an all-coefficient adaptive control method to stabilize a flexible rotor using an AMB. The performance of the controller was comparable those obtained with the benchmark  $\mu$ -synthesis controller. Zhao et al. (2015) used model predictive control (MPC) method to study the stability of a flexible rotor – AMB system subject to the input and output constraints. Fang et al. (2015) tested a damping control method on a 315 kW magnetically suspended rotor which reduced the rotor 1X amplitude near the critical speed.

Enemark and Santos (2016) achieved significant reduction in 1X vibration force of a magnetically suspended centrifugal compressor with an adaptive notch filter. Zheng and Feng (2016) devised an adaptive notch filter to eliminate the current stiffness force of a magnetically suspended centrifugal compressor using a compensation signal. Significant reduction in synchronous vibration force is achieved at 30,000 rpm in experiments.

Lusty et al. (2014, 2016) developed a concentric twin–spool rotor consisting of a hollow outer rotor mounted on bearings and coupled magnetically to inner non-rotating shaft in a clamped configuration. AMBs are activated at critical speeds of primary shaft resulting in a coupling between the two rotors that changes the vibration behaviour of the rotor system. Roy et al. (2016) implemented a control law called high-frequency band-limited PD control law on a rigid rotor-shaft system. This was shown to be more efficient compared to PID in reducing the rotor vibration amplitudes. Ranjan and Tiwari (2020) used auxiliary AMB to introduce virtual trial unbalances in a flexible rotor supported on rolling element bearings. Influence coefficients were calculated based on these trial unbalances and were used to balance rotor below its first critical speed.

Mani et al. (2006), Quinn et al. (2005) used multiple scales analysis to estimate a combination resonance among critical shaft frequencies, shaft rotational speed, and external frequency of AMB excitation. Sawicki et al. (2008), and Sawicki (2009) present similar experimental results on combination frequencies technique. Storozhev (2009) conducted experiments where in cracked rotor was supported/ levitated using AMBs unlike the earlier work where AMB was used as an exciter and not as a support.

Kasarda et al. (2007) performed experimental studies on the use of AMB to as an actuator for identifying shaft crack. Litak et al. (2009), Friswell et al. (2010) used recurrence plots to study the condition of a cracked rotor. Sawicki et al. (2011a, 2011b) used combination frequencies to study the response of a cracked rotor system excited by unbalance force and external AMB force. They used harmonic balance method instead of multiple scales analysis in their studies. Morais et al. (2012) numerically studied a phenomenon called self-healing wherein a mid-span AMB was used to control the breathing mechanism of crack. This however was found to increase the rotor vibration level.

Chasalevris and Papadopoulos (2015) used AMBs for early detection of shallow cracks (< 5% of shaft radius) in rotating shafts. Singh and Tiwari (2015, 2016) numerically studied the behaviour of a rotor-bearing-AMB system with a breathing crack. The vibration data that was lost on account of using AMB was compensated for by the use of controller current. Both vibration and AMB current were used for the purpose of identifying crack parameters. Sarmah and Tiwari (2018, 2020) identified internal and external damping coefficients in a cracked rotor system supported on auxiliary AMBs.

Chasalevris et al. (2011, 2014) used AMB to study the operation of worn out journal bearings. Xu et al. (2016) used a mid-span AMB exciter to study the bearing outer race defects of faulty rolling element bearings. Guinzburg and Buse (1995), Baun and Flack (1999) made direct measurements of reaction forces acting on centrifugal pump impellers with the help of retrofitted AMBs. Marshall et al. (2001) made static force measurement in AMBs using multi-point technique based on actuator geometry and control current. Raymer and Childs (2001) measured the force exerted by AMB on rotor using fibre-optic strain gages (FOSG) mounted on the magnetic poles.

Nordmann and Aenis et al. (2004) compared various AMB force measurement techniques such as i-s method, reluctance network method, and flux based method using Hall sensors. Zutavern and Childs (2008) identified the parameters of an annular gas seal on a flexible rotor test rig using AMBs. The dynamic forces acting on the rotor were measured using four fibre-optic strain gauges and further used for parameter identification. Kozanecka et al. (2008) used measured gaps and measured magnetic forces to estimation of the bearing dynamic parameters. Tiwari and Chougale (2014) developed a linear regression algorithm for the estimation of AMB dynamic parameters and rotor unbalances for a flexible rotor system levitated on AMBs. The numerically estimated parameters were compared with the previously obtained experimental results obtained by Tiwari et al. (2009). Tiwari and Viswanadh (2015) estimated stiffness constants of AMBs and residual unbalances in a rigid rotor system levitated on AMBs using the numerical responses obtained from a Simulink™ model.

After conducting a comprehensive survey of literature available on AMBs some gaps have been found which need to be explored. a) The comparison of the vibration characteristics of AMBs and Squeeze film dampers (SFD) has not been addressed. b) The identification of fault parameters in the presence of multiple faults such as unbalance, cracks, misalignment, rubs has not been investigated. c) The effect of AMB in rotor systems where lateral and torsional vibration is coupled has not been investigated.

### 3. Objectives

The objectives of the present work are

- a) To develop the mathematical model a rotor bearing system supported on SFDs (Rotor-1).
- b) To develop the mathematical model a rotor bearing system supported on AMBs (Rotor-2).
- c) To build the Simulink models for rotor-1 and rotor-2 to generate responses in time domain
- d) To perform parametric studies on rotor-1 by varying the geometric parameters of SFD such as clearance, land length.
- e) To perform parametric studies on rotor-2 by varying the gain constants of AMB ( $K_p$ ,  $K_i$ , and  $K_D$ ).
- f) To perform comparative study from the vibration responses of rotor-1 and rotor-2.

### 4. System Configuration and Mathematical Modeling

For the present study two different rotor-systems have been considered. Fig-2 shows the simply supported rotor- system with two discs supported on rolling element bearings at either end. Viscous damping is provided by incorporating squeeze film dampers at both the bearing locations. Figure 3 shows the same rotor- system supported on AMBs at either end.

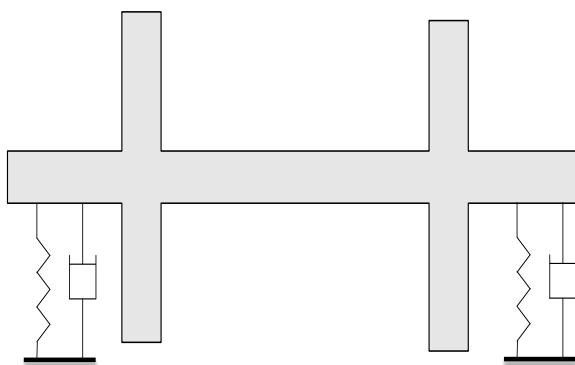


Fig-2: Rotor-Bearing-SFD system.

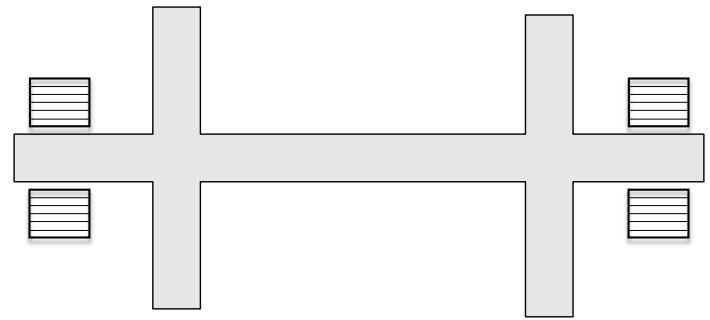


Fig-3: Rotor-AMB system.

#### 4.1 Shaft and disc model

In this work Timoshenko beam finite elements have been used to discretize the rotor system. The elemental matrices of size given in Chen and Gunter (2007) that correspond to a complex nodal displacement vector have been used for modeling each finite element. Besides reducing the computational effort.

$$\mathbf{u}^e = \mathbf{u}_{xz} + j\mathbf{u}_{yz} = \{x_1 \ \varphi_{y_1} \ x_2 \ \varphi_{y_2}\}^T + j\{y_1 \ \varphi_{x_1} \ y_2 \ \varphi_{x_2}\}^T \quad (1)$$

The mass, stiffness and gyroscopic matrices of shaft, discs are given in the Friswell et al. (2010).

#### 4.2 Force due to stiffness and damping of bearings

Rolling element bearings are isotropic with no cross-coupled stiffness coefficients. If  $k_{rad}$  is the radial stiffness of the bearing then the force vector due to stiffness is

$$\mathbf{f}_{b_{k_i}} = \begin{Bmatrix} 0.5(k_{rad}(u_{b_i} + \bar{u}_{b_i}) + k_{rad}(u_{b_i} - \bar{u}_{b_i})) \\ 0 \end{Bmatrix} \quad (2)$$

Generally the equivalent viscous damping of rolling element bearings is much lower than that of journal bearings. If  $c_{rad}$  is the radial stiffness of the bearing then the force vector due to damping is given by

$$\mathbf{f}_{b_{c_i}} = \begin{Bmatrix} 0.5(c_{rad}(\dot{u}_{b_i} + \dot{\bar{u}}_{b_i}) + c_{rad}(\dot{u}_{b_i} - \dot{\bar{u}}_{b_i})) \\ 0 \end{Bmatrix} \quad (3)$$

#### 4.3 Squeeze Film Damper

SFDs are commonly used in rotor systems in conjunction with a rolling element bearing for the purpose of attenuating rotor vibration. The empirical relations provided here are for the short bearing approximation (Chen & Gunter, 2007). When the oil film completely fills ( $2\pi$  film, no cavitation) the annulus then the stiffness and damping of SFD are given by

$$K = 0 \quad (4)$$

$$C = \frac{\mu RL^3 \pi}{C^3 (1 - \varepsilon^2)^{3/2}} \quad (5)$$

When the oil film partially fills the annulus ( $\pi$  film, cavitation) then the stiffness and damping of SFD are given by

$$K = \frac{2\mu RL^3 \varepsilon \omega}{C^3 (1 - \varepsilon^2)^2} \quad (6)$$

$$C = \frac{\mu RL^3 \pi}{2C^3 (1 - \varepsilon^2)^{3/2}} \quad (7)$$

where  $\mu$  is the viscosity of oil,  $C$  is the SFD clearance,  $\varepsilon$  is the eccentricity ratio ( $e/c$ ;  $e$  is the journal eccentricity),  $\omega$  is the angular speed of rotor,  $R$  is SFD radius and  $L$  is SFD land length. The above expressions are valid for the cases of circular synchronous radial motion about the origin with no precession.

#### 4.4 Active Magnetic Bearing

The lateral force exerted by the AMB on the rotor at its nodal location is given by

$$\mathbf{f}_{AMB} = \begin{Bmatrix} k_s u_{AMB} - k_i i_c \\ 0 \end{Bmatrix} \quad (8)$$

where

$$i_c(t) = K_p u_{AMB} + K_i \int u_{AMB} dt + K_D \dot{u}_{AMB} \quad (9)$$

$u_{AMB}$  is the complex rotor vibration at the AMB location,  $i_c$  is the complex AMB current  $k_s$  and  $k_i$  are the displacement and current stiffness constants of AMB.

In the present work PID control law is employed and the values of proportional gain ( $K_p$ ), integral gain ( $K_i$ ), derivative gain ( $K_D$ ) of the controller are taken from Bordoloi and Tiwari (2013). These gain values can be chosen from the pidTuner which is a MATLAB tuning algorithm with a graphical user interface.

#### 4.5 Unbalance Force

The unbalance force vector due to the mass eccentricities at the nodal locations of discs is

$$\mathbf{f}_{unb} = m_d e \omega^2 e^{j\omega t} e^{j\beta} \quad (10)$$

Where  $e$  is the disc unbalance eccentricity located at the phase angle  $\beta$ .

#### 4.6 Global Equations of Motion

For the case of rotor supported on SFDs the global EOM in complex form obtained by assembling the sub system matrices is given by

$$\mathbf{M}\ddot{\mathbf{u}} + (\mathbf{C} - j\omega\mathbf{G})\dot{\mathbf{u}} + \mathbf{K}\mathbf{u} = \mathbf{f}_{unb} \quad (11)$$

where

$$\mathbf{M} = \mathbf{M}_{shaft} + \mathbf{M}_{disc}; \mathbf{C} = \mathbf{C}_{brg} + \mathbf{C}_{SFD} + \mathbf{C}_{shaft};$$

$$\mathbf{K} = \mathbf{K}_{brg} + \mathbf{K}_{shaft}; \mathbf{G} = \mathbf{G}_{shaft} + \mathbf{G}_{disc}$$

For the case of rotor supported on AMBs the global EOM in complex form obtained by assembling the sub system matrices is given by

$$\mathbf{M}\ddot{\mathbf{u}} + (\mathbf{C} - j\omega\mathbf{G})\dot{\mathbf{u}} + \mathbf{K}\mathbf{u} = \mathbf{f}_{unb} + \mathbf{f}_{AMB} \quad (12)$$

where

$$\mathbf{M} = \mathbf{M}_{shaft} + \mathbf{M}_{disc}; \mathbf{C} = \mathbf{C}_{brg} + \mathbf{C}_{shaft}; \mathbf{K} = \mathbf{K}_{brg} + \mathbf{K}_{shaft};$$

$$\mathbf{G} = \mathbf{G}_{shaft} + \mathbf{G}_{disc}$$

#### 4.7 Simulink Model

Eq.(11) is used to build the Simulink model of Rotor-Bearing-SFD system shown in Figure 4. The responses of bearings, discs can be plotted using the time domain output of this model. Likewise Eq.(12) is used to build the Simulink model shown in Fig-5. In addition to the vibration responses at various axial locations along the length of the rotor, AMB current is also obtained from the model.

There are various fixed-step and variable-step solvers available in Simulink library. The choice of the solver depends upon the nature of the equations being solved. For the present problem Runge-Kutte 4<sup>th</sup> order solver with a fixed time step of  $10^{-4}$  s is used to solver Eq.(11) and Eq.(12).

The present section dealt with the development of mathematical models for Rotor-Bearing-SFD system and Rotor-AMB system using the elemental matrices of shaft, disc, and bearings. The external forces acting on the rotor system are the unbalance forces generated due to the uneven mass distribution. Simulink models have been developed for Rotor-SFD system and Rotor-AMB system to identify resonances and generate vibration responses in time domain. The AMB that is integrated with the rotor system works on PID control law. The next section deals with the

parametric studies and results generated from the Simulink models.

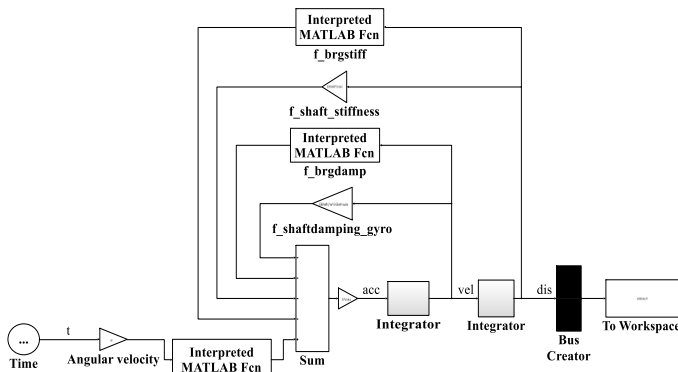


Fig-4 : Simulink model of Rotor-Bearing-SFD system (rotor-1)

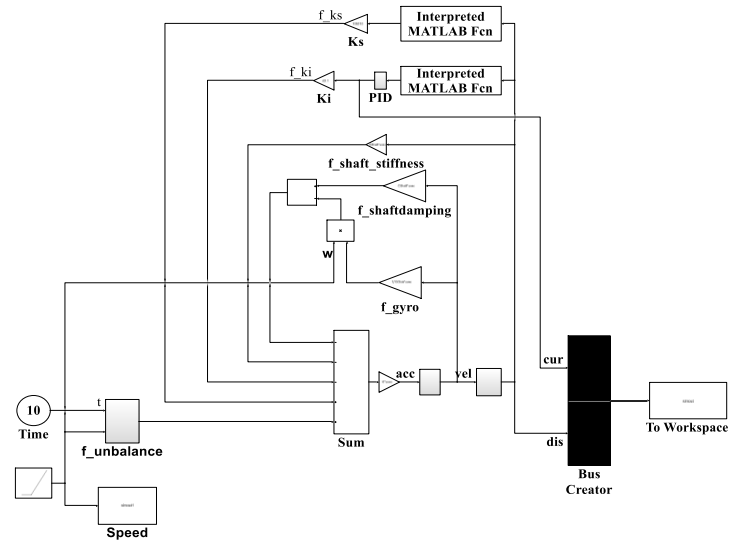


Fig-7: Simulink model of Rotor-AMB system for identifying resonances (rotor-2)

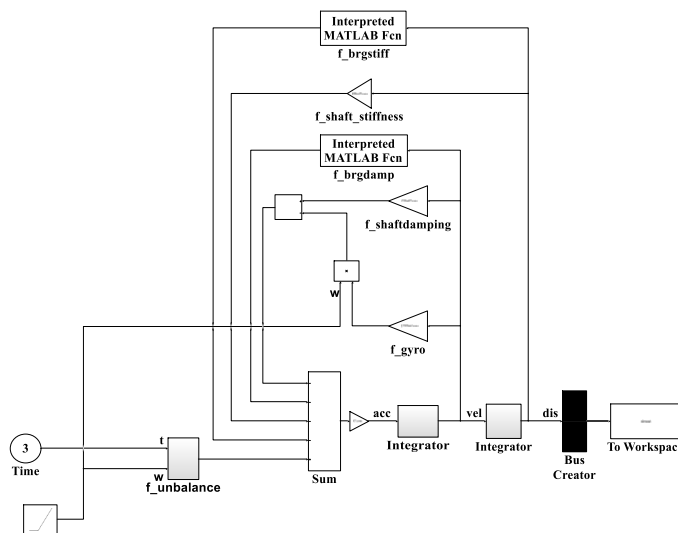


Fig-5: Simulink model of Rotor-Bearing-SFD system (rotor-1) for identifying resonances

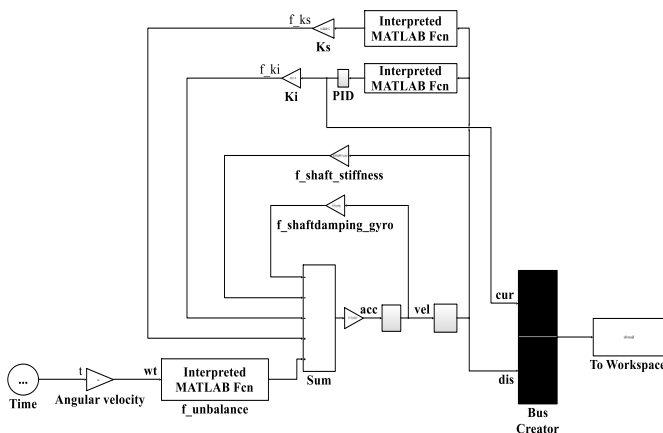


Fig-6: Simulink model of Rotor-AMB system (rotor-2)

### 5. Results and Discussions

In this section firstly the response of the rotor-bearing system without external viscous damping through SFD is studied. The rotor is discretized into 25 elements, each 20 mm in length. The nodal locations of bearings are (1, 21) and those of discs are (6, 21). Table 1 shows the geometric properties of the shaft, discs and bearings.

Table-1: Properties of shaft, discs, and bearings

Discs		Bearings			
$m_{d1}$ , kg	1	$k_{b1}$ , N/m	$4 \times 10^5$		
$m_{d2}$ , kg	1.27	$c_{b1}$ , N-s/m	300		
$I_{d1}$ , kg-m <sup>2</sup>	0.0011	$k_{b2}$ , N/m	$4 \times 10^5$		
$I_{d2}$ , kg-m <sup>2</sup>	0.0017	$c_{b2}$ , N-s/m	500		
$I_{p1}$ , kg-m <sup>2</sup>	0.0022	Unbalance			
$I_{p2}$ , kg-m <sup>2</sup>	0.0034	$m_1 e_1$ , kg-m	$4 \times 10^{-5}$	$m_2 e_2$ , kg-m	
				$3.8 \times 10^{-5}$	
Shaft		$\beta_1$ , rad	$\pi/6$	$\beta_2$ , rad	$\pi/3$
$d$ , m	0.02				
$l$ , m	0.5				

The critical speeds of the rotor system are obtained from Fig-8 which is the hilbert envelope of vibration in x direction that is obtained by ramping up the rotor from 0 rpm to 12000 rpm at a rate of  $40\pi$  rad/s for 10 seconds. It can be seen from that the resonant speeds of rotor are present at 3090 rpm and 8234 rpm. The orbits of the rotor at critical speeds are shown in Fig-9.

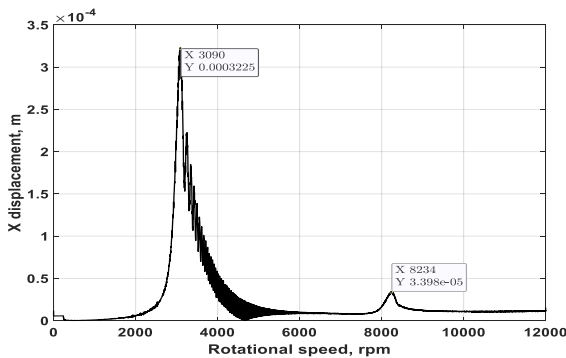


**Fig-8:** Hilbert envelope of rotor vibration in x direction for nominal unbalance at node-21

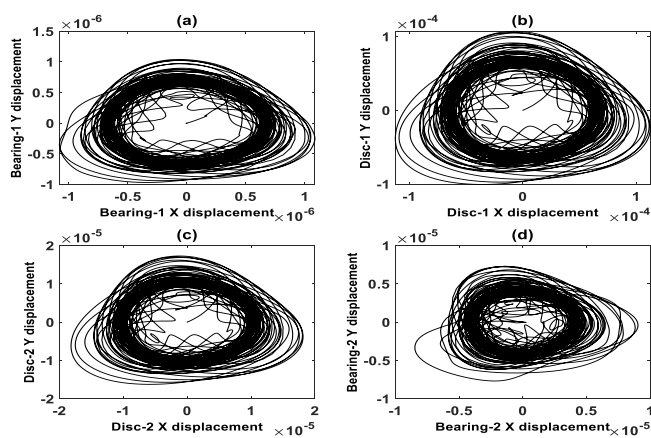


**Fig-9:** Orbits at various locations (a) Bearing-1 (b) Disc-1(c) Disc-2 (d) Bearing-2 for nominal unbalance

**5.1 Response of rotor system with squeeze film damper (rotor-1)**

Parametric studies are carried out by varying the radial clearance ( 125  $\mu\text{m}$ , 150  $\mu\text{m}$  and 200  $\mu\text{m}$ ) and land width of the SFD ( 20 mm, 25 mm). A  $2\pi$  oil film ( no cavitation) is assumed to be present around the annulus of the SFD. The damping coefficients are calculated from Eq.(5). The various parameters of SFD are given in Table 2.

**Table: 2** Parameters of Squeeze Film Damper

Oil viscosity, $\mu$ , N-s/m <sup>2</sup>	5e-3
SFD radius, R, mm	75
Land width, L, mm	20, 25
Radial clearance, c, $\mu\text{m}$	125, 150, 200

In practice SFDs operate at eccentricity ratios of 0.4 – 0.5. From Figures 10 (a) to 10(f) it can be seen that for a given land width with increasing clearance damping coefficient increases. Also it can be seen that for a given amount of radial clearance the damping value increases with increased land width. Fig-11 and Fig-12 show the orbits at various

locations along the rotor length i.e. at the locations of bearing-1, disc-1, disc-2 and bearing-2. It is clearly evident that higher damping contributes to a clear decrease in the size of the orbits. Fig-13 shows the response at disc-2 location for the above six configurations when the rotor accelerates from stand still to beyond second critical speed. Fig-14 shows that as damping increases the critical speeds shift to higher values. The amplitude of vibration decreases initially with increase in damping. Beyond a certain value of damping the amplitude again increases. The x displacement with  $c = 14510$  N-s/m is 400  $\mu\text{m}$  whereas with  $c = 28870$  N-s/m the x displacement is 500  $\mu\text{m}$ . This shows that increase in damping beyond a certain value rigidifies the support and leads to increase in vibration.

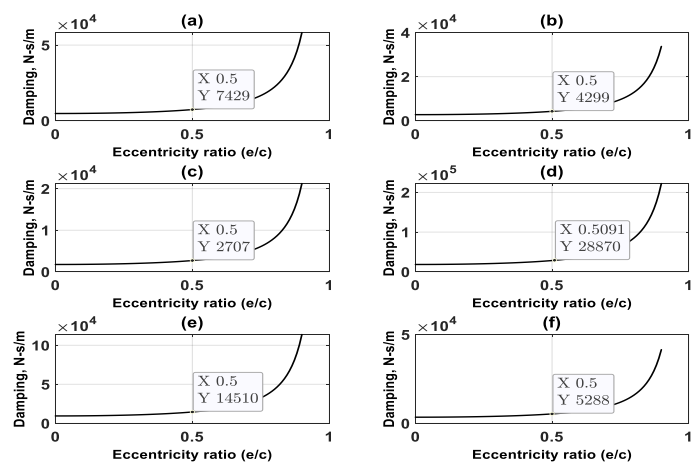


**Fig-10:** Damping coefficient vs eccentricity ratio for (a)  $c = 0.1$ ,  $L = 20$  (b)  $c = 0.125$ ,  $L = 20$  (c)  $c = 0.175$ ,  $L = 20$  (d)  $c = 0.1$ ,  $L = 25$  (e)  $c = 0.125$ ,  $L = 25$  (f)  $c = 0.125$ ,  $L = 175$  (c & L in mm)

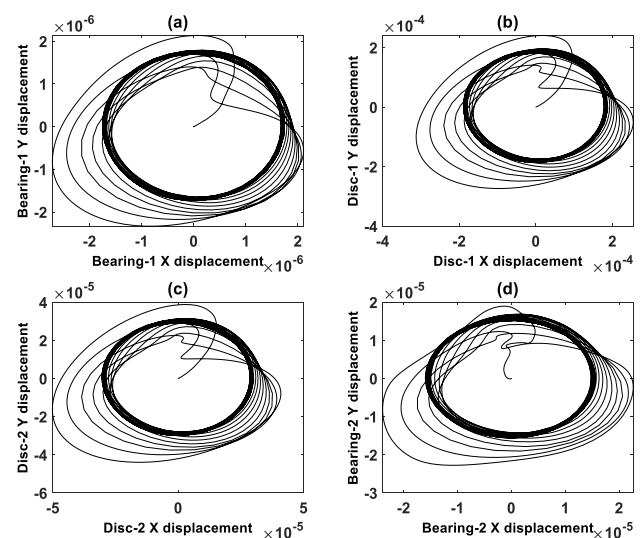


**Fig-11:** Orbits at various locations (a) Bearing-1 (b) Disc-1

(c) Disc-2 (d) Bearing-2 for  $c = 7430$  N-s/m

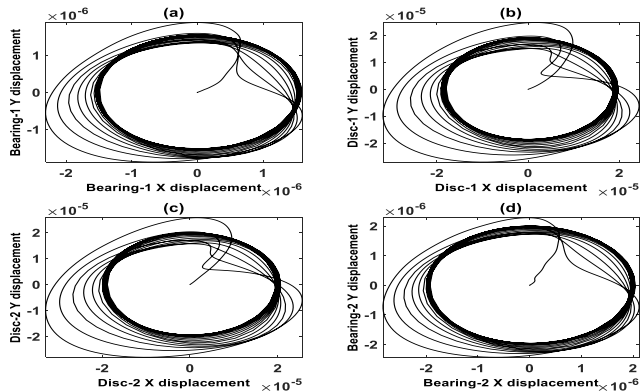


Fig-12: Orbits at various locations (a) Bearing-1 (b) Disc-1 (c) Disc-2 (d) Bearing-2 for  $c = 14510$  N-s/m

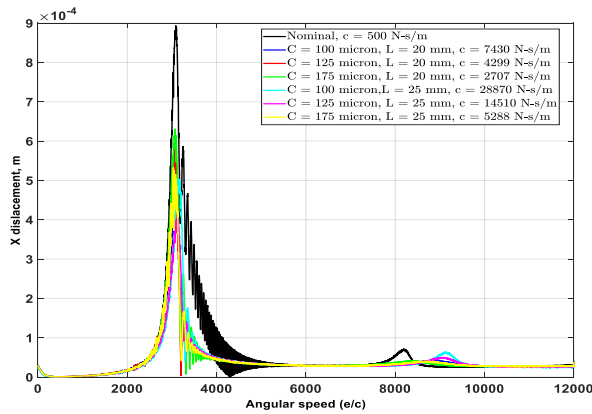


Fig-13: Response of various SFD configurations at Disc-2 location for 10 cm.gm unbalance

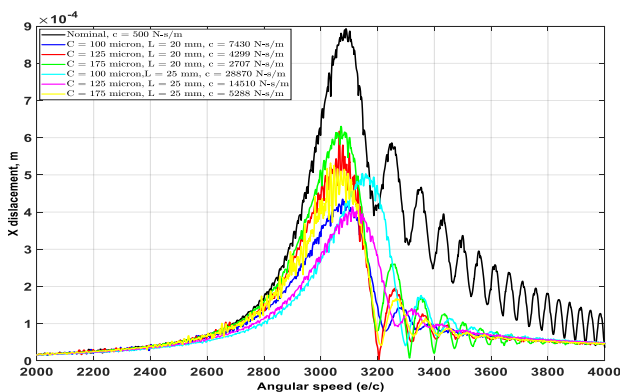


Fig-14: Response of various SFD configurations at 1st critical speed for 10 cm.gm unbalance

### 5.2 Response of rotor system with active magnetic bearing (rotor-2)

In the next stage parameteric studies are carried out by varying the gains  $k_p, k_i, k_D$  of controller to investigate their

effect of the responses. The values of AMB gains and AMB displacement stiffness and current stiffness are given in Table 3.

Table-3: AMB parameters considered for parametric studies

$k_p$	12000	8000	4000
$k_i$ , N/A	2000	1000	500
$k_D$	10	5	3
$k_s$	105210	$k_i$	42.1

From Fig-15 it can be seen that with increasing proportional gain  $k_p$  the critical speed of the rotor system shifts to higher speeds and increases the response amplitude as well. For  $k_p$  of 400 the critical speed and disc-1 amplitudes are 1056 rpm and 204 microns respectively. Increasing  $k_p$  to 12000 increases the respective values to 2045 rpm and 531 microns.

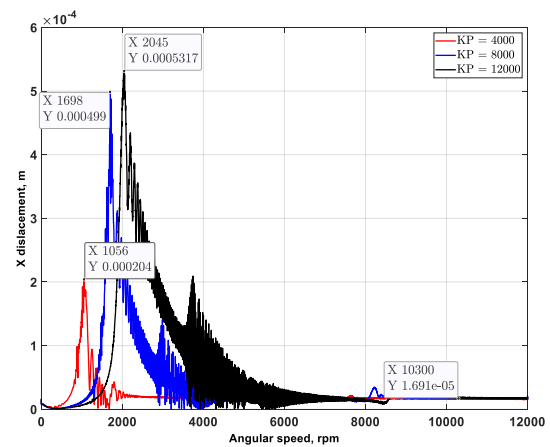


Fig-15: Sensitivity of Rotor-AMB system to  $k_p$  (x-displacement at Disc-1)

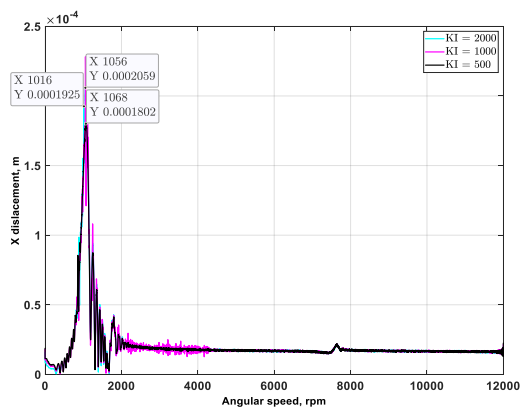


Fig-16: Sensitivity of Rotor-AMB system to  $k_I$  (x-displacement at Disc-1)

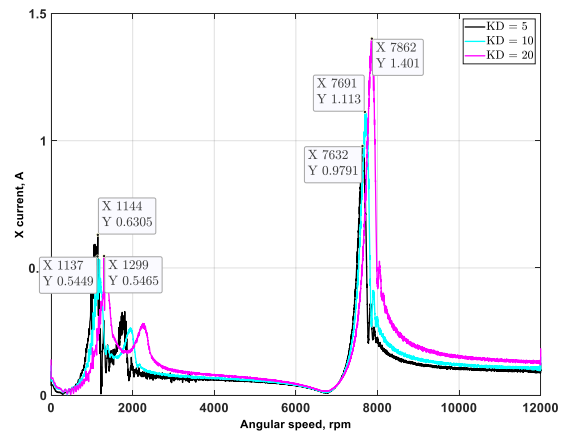


Fig-19: Sensitivity of Rotor-AMB system to  $k_D$  (x-current at Bearing 1)

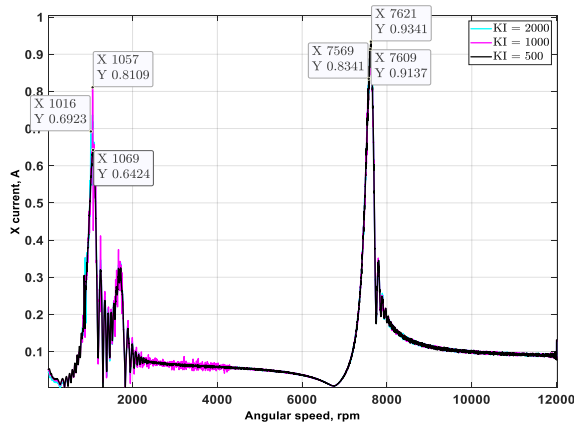


Fig-17: Sensitivity of Rotor-AMB system to (x-current at Bearing 1)

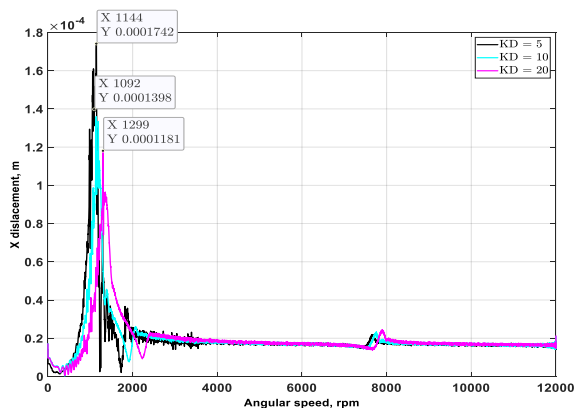


Fig-18: Sensitivity of Rotor-AMB system to  $k_D$  (x-displacement at Disc-1)

Fig-16 shows the effect of increasing Integral gain  $k_I$ . With increase in  $k_I$ , the response initially increases with increasing  $k_I$  and then decreases. Similar trend can be noticed in the critical speeds with the value shifting from 1068 rpm with  $k_D$  of 5 to 1056 rpm for a  $k_D$  value of 20 and then decreasing to 1016 rpm for a  $k_D$  value of 20. Fig-17 shows a similar trend in the AMB current plots. Fig-18 shows the effect of increasing derivative gain  $k_D$ . As the value of  $k_D$  increases from 5 to 20 the response amplitude decreases from 17 microns to 11 microns. The corresponding AMB current increases from 0.97 A to 1.4 as shown in Fig-19. Also a marginal shift in 1<sup>st</sup> critical speed can be noticed from 1144 rpm to 1299 rpm and the 2<sup>nd</sup> critical speed shifts from 7632 rpm to 7832 rpm.

## 6. Conclusions

A parametric study has been made to study the effect of incorporating squeeze film dampers and active magnetic bearings in a simple rotor system with two discs. Timoshenko beam elements are used to discretize the rotor system into finite elements. External forcing due to the mass unbalance present in the discs has been considered. The global equations of motion have been assembled using the mass, stiffness, gyroscopic matrices of shaft, mass and gyroscopic matrices of discs. Initially the response of rotor system with nominal damping has been considered. The 1<sup>st</sup> and 2<sup>nd</sup> critical speeds have been found to be present at 3090 rpm and 8234 rpm. The response at 1<sup>st</sup> critical speed is 322 microns. Next SFDs have been incorporated at bearing locations to introduce external viscous damping. Three different clearances and three different damper lengths have been considered for parametric studies. It has been shown that damping is linear up to an eccentricity ratio of 0.5. Beyond this it shows significant nonlinearity. From the response plots it is found that incorporation of SFD certainly

helps in vibration attenuation. However vibration amplitude decreases with damping only up to a certain value of damping coefficient. Beyond this value the damper locks up and behaves like a rigid support which leads to increase in vibration amplitude. . This goes to show that only properly tuned SFDs are helpful in vibration reduction. Next AMBs are incorporated at bearing locations. The effect of varying proportional, integral and derivative gains on the vibration amplitudes has been studied. Proportional gain helps in shifting the resonant speeds, however the peak at the resonant speed also increases. Increasing integral gain shifts the resonant speed marginally. However a reduction in vibration amplitude is noticed. The same behaviour is noticed with an increase in the value of derivative gain. From the results it has been found that AMBs provide more flexibility in controlling the dynamic behaviour of rotor system by way of shifting critical speeds and controlling vibration amplitudes. Also with SFD a new design/tuning essentially involves a replacing existing component with new one. With AMB tuning can be performed by varying the gains without changing any hardware. This shows the potential of AMBs to replace SFDs in rotordynamic applications.

## REFERENCES

1. Bordoloi, D.J., Tiwari, R., Optimization of controller parameters of Active Magnetic Bearings in Rotor Bearing Systems, *Advances in Vibration Engineering*, 12, pp 319 – 327, 2013
2. Basaran, S., Sivrioglu, S., Okur, B., and Zergeroglu, E., 2011, "Robust  $H_{\infty}$  control of Flexible Rotor Active Magnetic Bearing System", 6th International Advanced Technologies Symposium, Elazig, Turkey, 39 – 43
3. Chasalevris, A.C., Dohnal, F., Markert, R., 2011, "Symptoms of Misaligned Worn Journal Bearings in Rotor Response under External Excitation by A Magnetic Bearing", *Proceedings of the ASME 2011 International Design Engineering Technical Conferences & Computers and Information in Engineering Conference, IDETC/CIE 2011*, August 28-31, Washington, DC, USA
4. Chasalevris, A.C., Dohnal, F., Chatzisavvas, I., 2014, "Experimental detection of additional harmonics due to wear in journal bearings using excitation from a magnetic bearing", *Tribology International*, Volume 71, 158–167
5. Chasalevris, A.C., Papadopoulos C.A., 2015, "Experimental detection of an early developed crack in rotor-bearing systems using an AMB", *International Journal of Structural Integrity*, Volume 6, Issue 2, 194 – 213
6. Chen, W.J., Gunter, E.J., 2007, "Introduction to Dynamics of Rotor-Bearing Systems", Trafford Publishing, Charlottesville, Virginia, 469 pages.
7. Das, A.S., Dutt, J.K., Ray, K., 2010, "Active vibration control of unbalanced flexible rotor–shaft systems parametrically excited due to base motion", *Applied Mathematical Modelling*, Volume 34, Issue 9, 2353–2369
8. Defoy, B, Alban, T, Jarir M., 2014, "Experimental Assessment of a New Fuzzy Controller Applied to a Flexible Rotor Supported by Active Magnetic Bearing", *ASME Journal of Vibration and Acoustics*, Volume 136, 051006-1 - 051006-8
9. Enemark, S., Santos, I.F., 2016, "Feed forward compensation control of rotor imbalance for high-speed magnetically suspended centrifugal compressors using a novel adaptive notch filter", *Journal of Sound and Vibration*, Volume 366, 1 – 14
10. Fang, J., Tang, E., Zheng, S., 2015, "Optimum Damping Control of the Flexible Rotor in High Energy Density Magnetically Suspended Motor", Volume 137, 082505-1 - 082505-9
11. Friswell M.I., Penny, J.E.T., Garvey, S.D., Lees, A.W., *Dynamics of Rotating Machines*, Cambridge University Press, 1st Edition, March, 2010, New York, USA
12. Kasarda, M.E.F., Bash, T., Quinn, D., Mani, G., Inman, D., Kirk, R. G., 2007, "A New Approach for Health Monitoring and Detection of a Shaft Crack Using an Active Magnetic Actuator during Steady-State Rotor Operation", *Proceedings of GT2007, ASME Turbo Expo 2007: Power for Land, Sea and Air*, Montreal, Canada
13. Kozanecka, D., Kozanecki, Z., Lech, T., 2008, "Experimental Identification of Dynamic Parameters for Active Magnetic Bearings", *Journal of Theoretical and Applied Mechanics*, 46, 1, 41-50
14. Kozanecka, D., Kozanecki, Z., Lagodzinski, J., 2011, "Active magnetic damper in a power transmission system", *Commun Nonlinear Sci Numer Simulat*, Volume 16, Issue 5, 2273–2278
15. Litak, G., Sawicki, J.T., Kasperek, R., 2009, "Cracked rotor detection by recurrence plots", *Non-destructive Testing and Evaluation*, Volume 24, No. 4, 347–351
16. Mani, G., Quinn, D.D., Kasarda, M.E.F., 2006, "Active health monitoring in a rotating cracked shaft using active magnetic bearings as force actuators", *Journal of Sound and Vibration*, Volume 294, Issue 3, 454–465
17. Morais T S., Steffen, V. Jr., Mahfoud, J., 2012, "Control of the breathing mechanism of a cracked rotor by using electromagnetic actuator: numerical study", *Latin American Journal of Solids and Structures*, Volume 9, No. 5, 581 – 596
18. Nordmann, R., Aenis, M., 2004, "Fault Diagnosis in a Centrifugal Pump Using Active Magnetic Bearings", *International Journal of Rotating Machinery*, 10(3), 183–191
19. Quinn, D. D., Mani, G., Kasarda, M.E.F., Bash, T., Inman, D.J., Kirk, R. G., 2005, "Damage Detection of a Rotating Cracked Shaft Using an Active Magnetic Bearing as a Force Actuator-Analysis and Experimental Verification", *IEEE/ASME Transactions on Mechatronics*, Volume 10, No. 6, 640 – 647
20. Ranjan, G., Tiwari, R., 2020, "On-site high-speed balancing of flexible rotor-bearing system using virtual trial unbalances at slow run", *International Journal of Mechanical Sciences*, 183, 105786
21. Raymer, S.G., Childs, D.W., 2001, "Force Measurements in Magnetic Bearings using Fibre Optic Strain Gauges",

Proceedings of ASME Turbo Expo 2001 June 4-7, 2001, New Orleans, Louisiana

22. Roy, H.K., Das A.S., Dutt J.K., 2016, "An efficient rotor suspension with active magnetic bearings having viscoelastic control law", *Mechanism and Machine Theory*, Volume 98, 48-63

23. Sarmah, N., Tiwari, R., 2018, "Model based identification of crack and bearing dynamic parameters in flexible rotor systems supported with an auxiliary active magnetic bearing", *Mechanism and Machine Theory*, 122, 292-307

24. Sarmah, N., Tiwari, R., 2020, "Analysis and identification of the additive and multiplicative fault parameters in a cracked-bowed-unbalanced rotor system integrated with an auxiliary active magnetic bearing", *Mechanism and Machine Theory* 146,103744

25. Sawicki, J.T., 2008, "Rationale for Mu-Synthesis Control of Flexible Rotor-Magnetic Bearing Systems", *Acta Mechanica et Automatica*, Volume 2, No.2, 67 - 74

26. Sawicki, J.T., 2009, "Rotor Crack Detection using Active Magnetic Bearings", *Solid State Phenomena*, Volume 144, 9-15

27. Sawicki, J.T., Storozhev, D.L., Lekki, J.D., 2011, "Exploration of NDE Properties of AMB Supported Rotors for Structural Damage Detection", *ASME Journal of Engineering for Gas Turbines and Power*, Volume 133, 102501-1 - 102501-9

28. Sawicki, J.T., Friswell, M.I., Kulesza, Z., Wroblewski, A., Lekki, J.D., 2011, "Detecting cracked rotors using auxiliary harmonic excitation", *Journal of Sound and Vibration*, 330, pp. 1365 - 1381.

29. Schweitzer, G., Maslen, E.H., 2009, "Magnetic Bearings: Theory, Design and Application to Rotating Machinery", Springer-Verlag, Berlin, Heidelberg

30. Singh, S., Tiwari, R., 2015, "Model-based fatigue crack identification in rotors integrated with active magnetic bearings", *Journal of Vibration and Control*, 1 - 21

31. Singh, S., Tiwari R., 2016, "Model-based Switching-Crack Identification in a Jeffcott Rotor with an offset disk integrated with an Active Magnetic Bearing", *ASME Journal of Dynamic Systems, Measurement, and Control*, Volume 138, 031006-1 - 031006-11

32. Storozhev, D.L., 2009, "Smart Rotating Machines for Structural Health Monitoring", Thesis, Master of Science in Mechanical Engineering, Cleveland State University

33. Tiwari, R., Chougale, A., 2014, "Identification of bearing dynamic parameters and unbalance states in a flexible rotor system fully levitated on active magnetic bearings", *Mechatronics*, Volume 24, Issue 3, 274-286

34. Tiwari, R., Viswanadh, T., 2015, "Estimation of speed-dependent bearing dynamic parameters in rigid rotor systems levitated by electromagnetic bearings", *Mechanism and Machine Theory*, Volume 92, 100-112

35. Wang, Y., Fang, J., Zheng, S., 2014, "A Field Balancing Technique Based on Virtual Trial-Weights Method for a Magnetically Levitated Flexible Rotor", *ASME Journal of Engineering for Gas Turbines and Power*, Volume 136, 092502-1 - 092502-7

36. Xu, Y., Di, L., Zhou, J., Jin, C., Guo, Q., 2016, "Active magnetic bearings used as exciters for rolling element bearing outer race defect diagnosis", *ISA Transactions* 61, 221-228

37. Zhao, J., Zhang, H.T., Fan, M.C., Wu, Y., 2015, "Control of a Constrained Flexible Rotor on Active Magnetic Bearings", *International Federation of Automatic Control Papers Online*, Volume 48, Issue 28, 156-161

38. Zheng, S., Feng, R., 2016, "Feed forward compensation control of rotor imbalance for high-speed magnetically suspended centrifugal compressors using a novel adaptive notch filter", *Journal of Sound and Vibration*, Volume 366, 1-14

39. Zhong, Z.X., Zhu, C.S., 2013, "Vibration of flexible rotor systems with two-degree-of-freedom PID controller of active magnetic bearings", *Journal of Vibroengineering*, Volume 15, Issue 3, 1302 -310

40. Zutavern, Z.S., Childs, D.W., 2008, "Identification of Rotordynamic Forces in a Flexible Rotor System Using Magnetic Bearings", *ASME Journal of Engineering for Gas Turbines and Power*, Volume 130, 022504-1 - 022504-6